Astron. Astrophys. 349, 283–294 (1999)

ASTRONOMY AND ASTROPHYSICS

Observations of linear polarization in the H_α line during two solar flares

Etienne Vogt and Jean-Claude Hénoux

Observatoire de Paris-Meudon, DASOP, CNRS URA 2080 (Laboratoire de Physique du Soleil et de l'Héliosphère), 5 Place Jules Janssen, F-92195 Meudon Cedex, France

Received 19 June 1998 / Accepted 9 March 1999

Abstract. Two chromospheric flares were observed in Meudon using an H_α flare polarimeter on $17^{\rm th}$ July 1982 and $20^{\rm th}$ June 1989. A careful reduction of the data sets has been done in order to remove the false polarization signals induced by atmospheric turbulence. In each event, linear polarization directed towards the disk center with a polarization degree of the order of 5% is detected. This polarization is correlated in time with the maximum of soft X-ray emission. One event also shows polarization parallel to the solar limb at the moment of maximum hard X-ray emission but with a poor signal to noise ratio.

We interpret this polarization as impact polarization, resulting from the excitation of hydrogen atoms by anisotropic particles. The tangential polarization could be due to a beam of energetic electrons moving vertically. However, the best candidates to explain both tangential and radial polarization are beams of energetic protons with an energy below 100 keV entering into the chromosphere. The variation of the polarization direction could result from a modification of the magnetic topology during the flare.

Key words: Sun: flares – polarization – instrumentation: polarimeters

1. Introduction

Impact polarization has been observed before in solar flares. Hénoux et al. (1983a) have reported the observation of linear polarization in the S I 1437 Å UV line during a chromospheric flare on July 15, 1980, using the UVSP[1] instrument on the SMM[2] satellite. Later, Hénoux & Chambe (1990) and Hénoux et al. (1990) reported the observation of linear polarization in the H_α line during the July 11, 1982 flares, using the flare patrol polarimeter at Meudon Observatory. In both cases, the linear polarization observed was directed towards the disk center (radial polarization) and present during the flare gradual phase. It was interpreted as impact polarization by an anisotropic distribution of particles in the chromosphere. The time resolution of these polarization observations could not provide significant information on the H_α degree of polarization and orientation during the flare impulsive phase.

The absence of hard X-ray emission at the time where radial linear polarization was present ruled out energetic electrons as being responsible for its generation. The first source of anisotropy considered was a significant heat flux at the base of the transition zone (Hénoux et al., 1983b) that would create an anisotropic velocity distribution of 10 eV electrons. However, at chromospheric densities, the 10 eV electrons are quickly scattered by Coulomb collisions and do not keep a significant anisotropy down to the H_α formation layers. Thus, this hypothesis was abandoned.

Another possible origin is in photoelectrons expelled from the inner shells of atoms like C, N and O by soft X-ray irradiation. This hypothesis would naturally explain the association observed between soft X-ray emission and radial polarization. However, the expected degree of polarization is too low to explain the observations by photoelectron collisional excitation (see 5.2).

Protons are much less scattered by Coulomb collisions than are the low energy electrons, due to the energy degration of the energetic electrons at the origin of hard X-ray brehmsstrahlung, which are also able to excite the H_α line. Therefore, a beam of protons accelerated in the corona to an energy of a few hundred keV is able to reach the H_α formation layers without losing its directivity. Such low energy protons are currently the best candidates to explain the relatively high degree (5 to 10%) of linear polarization observed.

Linear polarization of the Balmer H_α line during two solar impulsive flares was also reported by Metcalf et al. (1992) and Metcalf et al. (1994). The direction of the polarization vector was found to be within 20 degree from the radial direction and was also interpreted as due to atmospheric bombardment by low energy protons.

The two chromospheric flares studied in this paper were observed in Meudon with the flare patrol polarimeter on July 17, 1982 and June 20, 1989. Preliminary results for these events were already published in Hénoux (1991) for the 1982 flare and in Vogt & Hénoux (1996) for the 1989 one. However, the seeing effects, which produce false polarization signals, were not completely taken into account in this preliminary work. Here, a

Send offprint requests to: E. Vogt

[1] Ultraviolet Spectrometer and Polarimeter

[2] Solar Maximum Mission

more extensive treatment of the noise induced by seeing effects is done. This allows a better determination of the observed polarization degree and azimuth that we can now compare with theoretical predictions (Vogt et al., 1997). In Sect. 2, what is currently known about protons in flares is described. In Sect. 3, the polarisation measurement technique used is described and in Sect. 4, the observations are presented. Finally, in Sect. 5, we discuss the origin of the polarization using the available theoretical results.

2. Protons in flares

It is generally accepted that electrons are accelerated during solar flares to energies of a few hundred keV as these energetic electrons are responsible for the observed hard X-ray bursts through the physical process known as *bremstrahlung* or free-free emission. On the other hand, protons accelerated to these energies do not directly emit any significant radiation and their potential role in flares was at first neglected.

There is indirect evidence in favour of a significant flux of protons below 1 MeV in solar flares. Simnett (1995) remarked that the hot plasma ($T \approx 10^7$ K) formed during flares is sometimes animated by ascending motions before the rise of hard X-ray emission. This is not compatible – for simple causality reasons – with the hypothesis that this hot plasma is formed by evaporation of chromospheric material bombarded by electron beams. These observations could be explained by a hundred keV proton beam bombardment that would start before the acceleration of electrons.

The more direct proof that protons above 1 MeV are indeed accelerated in solar flares comes from the observation of nuclear γ-ray lines such as the 1.63 MeV line of ^{20}Ne, the 4.4 MeV line of ^{12}C or the 6.1 MeV line of ^{16}O. These lines are emitted by nuclei excited by collision with highly energetic ions ($>$ 2 MeV). The 1.63 MeV line of ^{20}Ne is particularly bright in γ flares. This was first interpreted as due to a higher abundance of neon compared to other elements like carbon or oxygen. At this time, the proton energy spectrum used to explain the observed intensities of γ-ray lines was represented by Bessel functions that are roughly constant with energy below 2 MeV (Murphy et al., 1991).

Recently, Share & Murphy (1995) and Ramaty et al. (1995) suggested that a proton spectrum that continued to rise towards low energies could explain the observed intensity ratio of the ^{20}Ne and ^{16}O lines as the nuclear excitation cross section of ^{20}Ne has a maximum for energies of order of 5 MeV whereas the cross section of ^{16}O is only significant beyond 10 MeV.

So we have good reasons to think that protons with energy below 1 MeV (some hundreds of keV) are present in flares whether showing γ-ray lines emission or not. Such protons are difficult to detect directly as they do not emit any significant amount of X-rays. However, these proton beams could be detected indirectly at chromospheric level, through the effects of their collisions with background atoms. Spectropolarimetry is a valid diagnostic method for protons, as their heavy mass helps them to keep their directivity down to the chromosphere where they can generate linearly polarized line emission through impact polarization. It is the case for the H_α line that has been studied here at Paris-Meudon Observatory.

Electron acceleration is currently considered as the dominant process in the energetics of solar flares. If the proton energy spectrum was given by a power law down to energies of some hundreds of keV, the energy transported by protons in solar flares could be comparable, or even greater, than the energy transported by electrons. Therefore, the detection of low energy protons and an estimation of their number flux are of great significance for understanding the particle acceleration mechanisms in solar flares.

3. H_α linear polarization measurement technique

3.1. The Meudon H_α spectropolarimeter

The instrument used is a heliograph equipped with a Lyot filter tuned to the center of the H_α line. The bandwidth of the filter is 0.75 Å. A polarization analyser is placed in front of the entrance of the Lyot filter. It is composed of a rotating half-wave plate in front of a fixed linear polarizer. Since the polarization analyser is placed directly on the main optical axis, the instrumental polarization is very weak and can be neglected. A schematic representation of the instrument in the configuration used for the observations is presented in Fig. 1.

During the observations, the half-wave plate is rotated by steps of 22.5°. At each step, an H_α image is taken by a 35mm photographic camera, giving the spatial variation of $I-U$, $I+Q$, $I+U$ and $I-Q$ for four consecutive positions of the plate. The time interval between two exposures was 4 seconds, for the two observations described in this paper.

To retrieve the Stokes parameters I, Q and U, images are first digitized using a microdensitometer, then they are added and subtracted after compensation for image motions in the focal plane by cross-correlation techniques described in the next subsection. The linear polarization degree P and the azimuth Φ of the polarization vector are then given by:

$$P = \frac{\sqrt{Q^2+U^2}}{I}\,, \quad \tan 2\Phi = \frac{U}{Q} \tag{1}$$

A new version of the instrument called PARIS[3] is now available in Meudon. The bulk of the instrument is unchanged, but the 35mm photographic camera has been replaced by a 384 $\times$ 288 CCD electronic camera that will provide better sensitivity and time resolution and remove the need to digitize the images with a microdensitometer as the first data processing step.

3.2. Data reduction method

With this instrument, the polarization is obtained by combinations of images taken at different times. Therefore, time variations of brightness on the sun, seeing effects and image motions due to the rotating plate introduce noise into the polarization signal.

[3] Polarimeter for Active Regions Instabilities Study

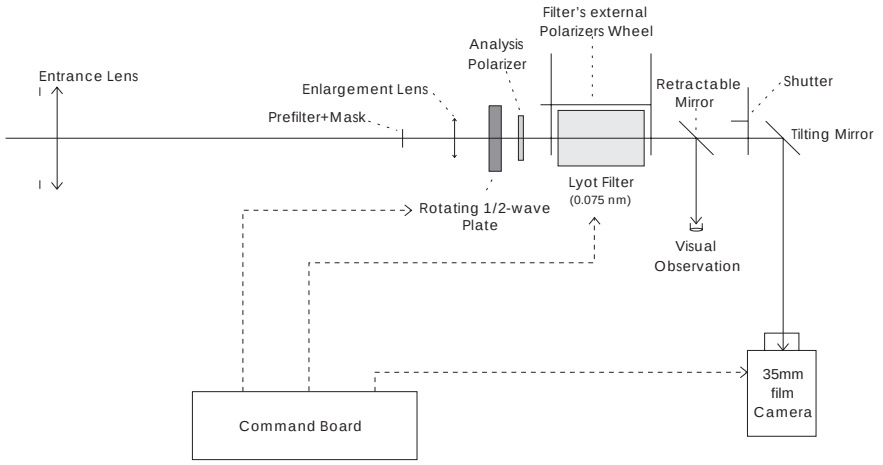

Fig. 1. Schematic representation of the H_α polarimeter in Meudon

The effect of the rotating half-wave plate is easy to correct. It induces global translations of the field of view that are compensated by image correlation software. The translation $(\Delta x, \Delta y)$ between two consecutive images i and $i+1$ is determined by minimizing the function S defined as:

$$S_i(\Delta x, \Delta y) = \sum_{n=1}^{n_z} \sum_{x=x_{min}^{(n)}}^{x_{max}^{(n)}} \sum_{y=y_{min}^{(n)}}^{y_{max}^{(n)}} (\mathcal{I}_i(x,y) - \mathcal{I}_{i+1}(x+\Delta x, y+\Delta y))^2 \quad (2)$$

where $\mathcal{I}$ are the observed intensities, n_z is the number of comparison areas used and $x_{min}^{(n)}$, $x_{max}^{(n)}$, $y_{min}^{(n)}$ and $y_{max}^{(n)}$ are the coordinates defining each comparison area in the reference image. These comparison areas are chosen to contain well contrasted details that are stable in time such as the solar limb, a sun spot or, by default, a flare kernel that does not evolve too fast.

The effects of the time variations of flare brightness can be reduced by using combinations of three consecutive images $\mathcal{I}$ to compute the Stokes parameters Q and U:

$$\begin{aligned} Q_1 &= 2\mathcal{I}_2 - \mathcal{I}_1 - \mathcal{I}_3 \quad (3)\\ U_1 &= 2\mathcal{I}_3 - \mathcal{I}_2 - \mathcal{I}_4 \\ Q_2 &= -2\mathcal{I}_4 + \mathcal{I}_3 + \mathcal{I}_5 \\ U_2 &= -2\mathcal{I}_5 + \mathcal{I}_4 + \mathcal{I}_6 \\ &\dots \end{aligned}$$

We can then express $\mathcal{I}_{n-1}$ and $\mathcal{I}_{n+1}$ as a function of $\mathcal{I}_n$, as a second order finite difference in the time interval Δt between two images:

$$\mathcal{I}_{n-1} = \mathcal{I}_n - \left(\frac{\partial \mathcal{I}}{\partial t}\right)_n \Delta t + \frac{1}{2}\left(\frac{\partial^2 \mathcal{I}}{\partial t^2}\right)_n \Delta t^2 \quad (4)$$

$$\mathcal{I}_{n+1} = \mathcal{I}_n + \left(\frac{\partial \mathcal{I}}{\partial t}\right)_n \Delta t + \frac{1}{2}\left(\frac{\partial^2 \mathcal{I}}{\partial t^2}\right)_n \Delta t^2 \quad (5)$$

Then we get:

$$\mathcal{I}_{n-1} + \mathcal{I}_{n+1} = 2\mathcal{I}_n + \left(\frac{\partial^2 \mathcal{I}}{\partial t^2}\right)_n \Delta t^2, \quad (6)$$

that shows that the contribution of the first time derivative of the intensity to the observed Stokes parameters Q and U vanish. However, this is not enough during fast variations of brightness such as those that occur during the impulsive phase of a flare. Thus, we should be cautious when looking at polarization data obtained during this phase.

Finally, seeing-induced effects are the most tricky ones as they cause unpredictable distortions of the images, mixing intensity into the polarization parameters (this is known as *seeing induced crosstalk*). Often seen effects of these distortions are opposite polarization signals appearing on either sides of a bright H_α patch. These correspond to polarization vectors whose azimuth differs by 90°. Such structures, easily identified on polarization maps or on azimuth distribution histograms, are a first indication of a noisy observation. As we are not able to remove the false polarization signals from our data, we use time and space integration to reduce the noise level and extract the real signal.

In the polarization data obtained from four consecutive images, the noise level is generally much higher than the expected polarization degree of 5 to 10%: single pixels can show a polarization degree of 20% with comparable fluctuations between consecutive polarization maps. To reduce this noise, the Stokes parameters are integrated in space and in time. Spatial integration combines 3×3 pixels into one, reducing both the amount of data and the single pixel fluctuations. We also do spatial integrations over all the active region, to study the global polarization degree as a function of time.

The first level of time integration combines the 3×3 spatially integrated Stokes images obtained during a complete rotation of the half-wave plate – roughly one minute of time – into single I, Q and U images. After these integrations, polarization degrees of the order of 5% clearly emerge from a noise level of the order of 2%, except during the impulsive phase of the flare, where the fast time variations of brightness produces a higher noise level.

To further reduce the noise, a second level of time integration is done over 4 to 12 minutes. This allows polarization degrees of the order of 2% to be clearly seen over a noise level down to 0.5–1% if the polarization is stable enough during the period of integration.

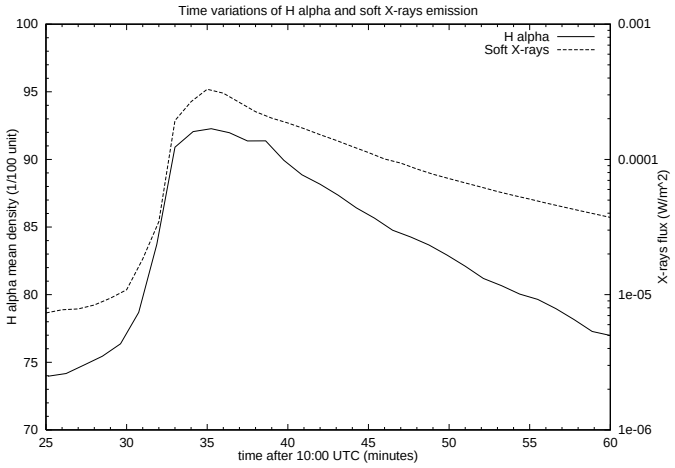

Fig. 2. Time evolution of the soft X-ray flux and H_α emission for the 1982, July 17 flare, from 10:25 to 11:00 UTC.

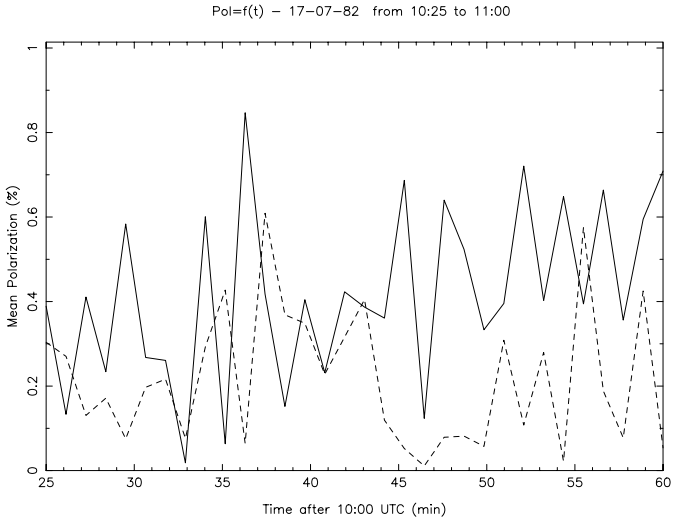

Fig. 3. Time evolution of the radial (plain line) and tangential (dotted line) components of the polarization integrated over the western flare of July 17^{th} 1982, from 10:25 to 11:00 UTC.

4. Observations

4.1. July 17$^{\rm th}$ *1982 flares*

Two solar flares were observed on July 17, 1982 in the same active region. The first one was located at 11°N, 38°W on the solar disk from 10:25 to 11:02 UTC. The second one, less bright than the first, was located at 17°N, 29°W from 10:32 to 11:02 UTC. Observations made by the Meudon polarimeter were digitized from 10:25 to 11:00, giving a total of 32 series of 16 images. This event was also accompanied by soft X-ray emission. There is no known emission of hard X-ray or γ-ray (no event is recorded on the SMM Hard X-ray Burst Spectrometer or Gamma Rays Spectrometer events lists).

4.1.1. Soft X-ray emission

This event was observed by the GOES[4] 2 satellite in two energy bands: 0.5–4 Å and 1–8 Å. The variation of the flux received in the 1–8 Å wavelength band is presented in Fig. 2, together with the H_α emission.

From 10:30 to 10:34, the X-ray flux rises by a factor 30 from its pre-flare value. The maximum is reached at 10:35 with a flux of $3\ 10^{-4}$ W.m^{-2}. Then, it decreases gradually.

4.1.2. H_α line intensity

For the study of the time variation of the H_α emission, we used the time-integrated intensity images. Those give in fact the photometric densities, that are related to the intensities by the relation:

$$d - d_0 = 1.35 \log_{10} \frac{I}{I_0} \qquad (7)$$

A mean density was computed by spatial integration over a rectangular area covering the western flare, the more intense of the two. Correction for the variations of atmospheric transparency was done by subtracting the density variations observed on a quiet region. The result is presented in Fig. 2, together with the soft X-ray emission to clearly show the similarities between the two curves.

On the H_α curve, we see a fast increase from 10:30 to 10:33. The maximum is reached at 10:35 and is followed by a gradual decrease. The correlation between the soft X-ray emission and the H_α emission from the western flare shows that this flare is the main event. The H_α emission from the eastern flare does not show this correlation (Vogt, 1997).

4.1.3. H_α line polarization

The H_α polarization was studied from 10:25 to 11:00 UTC, with a time resolution of 1, 4 and 12 minutes. On the eastern flare, the observed polarization does not show any stable orientation during time or over the area (Vogt, 1997). Furthermore, when we see polarization above the noise background of 1–2% in the 1 min integrated data, typical seeing-induced patterns are seen (opposite polarizations on either side of a bright patch). Therefore, in the following we consider only the western flare.

The one minute integrated data are very noisy, especially from 10:29 to 10:34, when the H_α emission varies rapidly (we will refer to that period as the "impulsive phase" of the flare, although there is no impulsive hard X-ray emission observed). The time profile of the area integrated polarization is represented in Fig. 3. The plain curve represents the radial polarization fraction (projection of the polarization vector along the flare to disk center direction). Its mean value over the event is 0.42% with a standard deviation of 0.21%. The dotted curve represents the tangential polarization (perpendicular to the radial one); its mean value is 0.22% with a standard deviation of 0.16%. The first impression we get is that, in spite of the large fluctuations, radial polarization seems to be dominant most of the time. If we consider peaks above 3 standard deviations to be significant

[4] Geostationary Operational Environmental Satellite

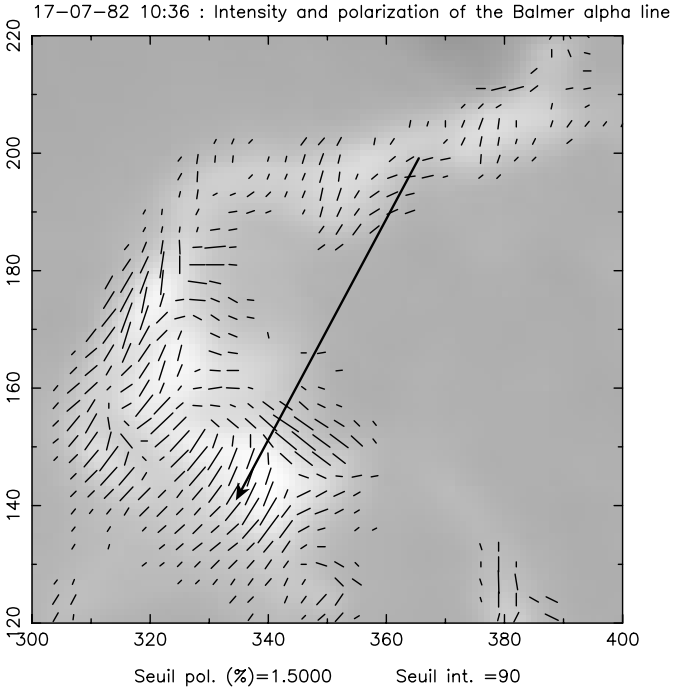

Fig. 4. H_α intensity and polarization exceeding 1.5% on the 1982, July 17 western flare at 10:36 UTC. The radial orientation is indicated by the big arrow; the units are in pixels ($\approx$ 1 arcsec).

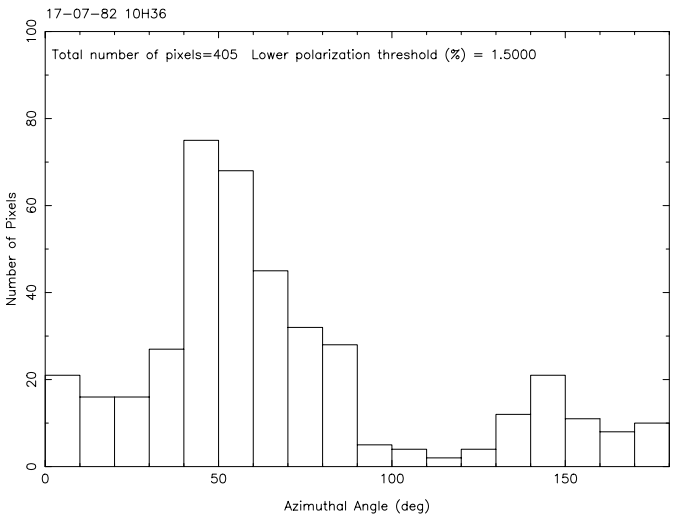

Fig. 5. Azimuth distribution of the one minute time integrated polarization exceeding 1.5% on the 1982, July 17 western flare at 10:36 UTC. The radial orientation is at 62° and the tangential one at 152°.

(0.6%), we see several peaks of clear radial polarization with the most prominent one at 10:36. Secondary peaks can be seen at 10:45, 10:47, 10:52, 10:54, 10:56 and 11:00. Some peaks also appear on the tangential polarization curve, but they all have a comparable value of the radial component, so this is not a clear tangential direction.

The polarization map and azimuth distribution histogram for 10:36 are shown in Figs. 4 and 5 respectively. They show a polarization clearly peaked in a direction close to radial which covers most of the flaring area. This clear radial polarization is observed at or just after the maximum of soft X-ray and H_α emission (within the time accuracy of the observations).

The polarization integrated over four minutes shows a preferred orientation close to the radial direction during most of the observation period, with the exception of the impulsive phase. Three of the four minute time-integrated histograms are shown in Fig. 6. The last two panels (10:43 to 10:46 and 10h47 to 10h51) show a clear peak at 15–20° from the radial direction. In the first panel (10:34 to 10:37), the preferred direction is less clearly defined as the polarization fluctuates more during that period. The polarization degree observed in these datasets is between 1 and 2%.

In the 12 minute time-integrated data, a preferred direction of polarization can still be seen after the soft X-ray maximum, but is is less clearly defined (Vogt, 1997).

4.2. June 20$^{\rm th}$ 1989 flare

A solar flare was observed on June 20, 1989 at 24°N and 68°W. Observations from the H_α polarimeter in Meudon were digitized from 14:54 to 15:19 UTC for a total of 20 series of 16 images. This event was accompanied by gradual soft X-ray emission and also by impulsive hard X-ray, γ-ray and radio emissions.

4.2.1. Soft X-ray and H_α line intensity

This event was observed in soft X-ray by the GOES 7 satellite in the two wavelength bands 0.5–4 Å and 1–8 Å. The variation of the flux received in the 1–8 Å band is presented in Fig. 7, together with the H_α emission. From 14:55 to 15:05, the X-ray flux rises by a factor 30 from its pre-flare value. The maximum is reached at 15:07 with a flux of $1.6\ 10^{-4}$ W.m^{-2}. Then, the soft X-ray flux decreases gradually.

The time variation of the H_α emission was studied in the same way as for the 1982 events. We see a fast increase from 14:54 to a maximum at 15:02 that is followed by a gradual decrease with a slight bump at 15:08, one minute after the maximum of soft X-ray emission. For this event, the time variations of H_α and soft X-ray emissions are not as strongly correlated as they were for the 1982 flare.

4.2.2. Hard X-ray, γ-ray and radio emissions

Hard X-ray and γ-ray were observed respectively by the HXRBS[5] and GRS[6] instruments on the SMM satellite. The hard X-ray emission (Fig. 8) starts at 14:54:30 and reaches a maximum around 14:57:30 with 2383 counts per second. The integrated flux for the event is 396 000 counts in the 52.2–858.5 keV energy band.

The γ-ray emission observed by GRS shows the same characteristics as the hard X-ray emission below 1 MeV. Above 1 MeV, the count rates are very low, which makes the nuclear

[5] Hard X-ray Burst Spectrometer
[6] Gamma-ray Spectrometer

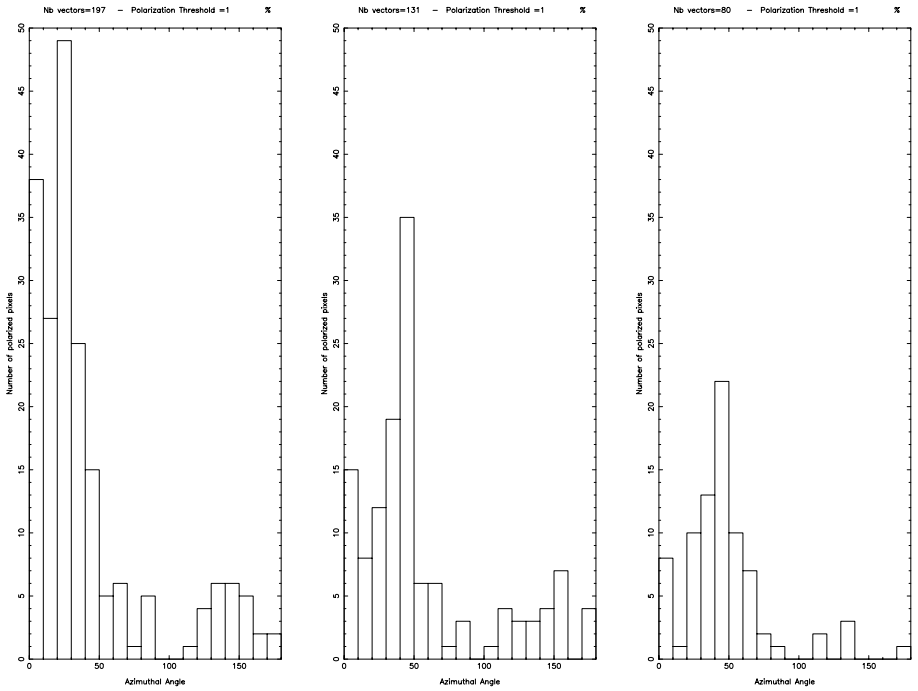

Fig. 6. Azimuth distribution of the 4 minute time-integrated polarization exceeding 1% on the 1982, July 17 western flare from 10:34 to 10:37, 10:43 to 10:46 and 10:47 to 10:50. The radial orientation is at 62° and the tangential one at 152°.

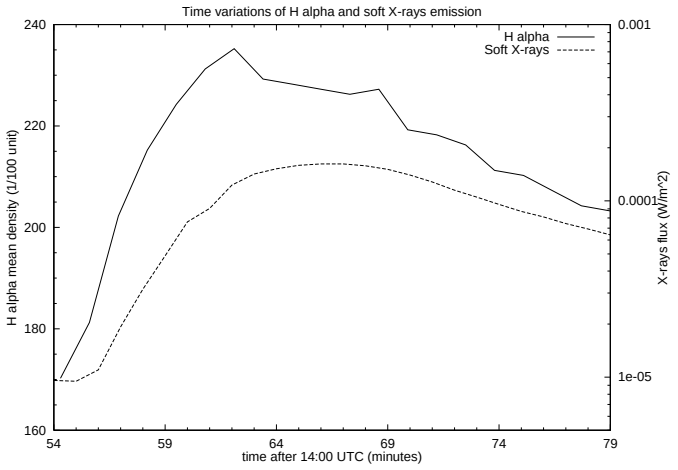

Fig. 7. Time evolution of the soft X-ray flux and H_α emission for the 1989, June 20 flare, from 14:54 to 15:19 UTC.

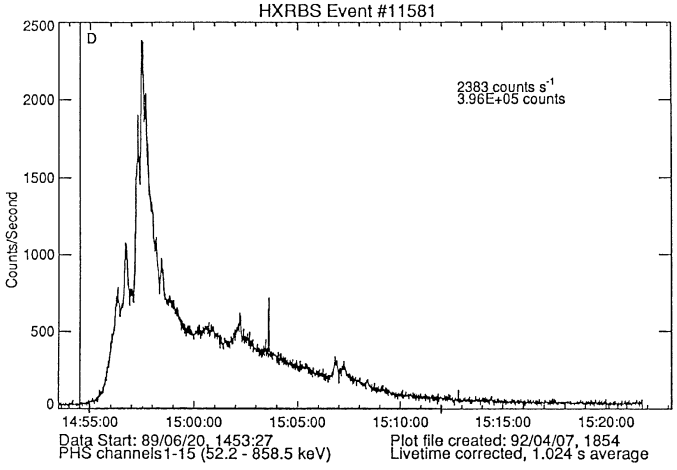

Fig. 8. Time evolution of the hard X-ray emission (52.2–858.5 keV) for the 1989, June 20 flare, from 14:54 to 15:22 UTC.

lines excited by high energy protons extremely difficult to see. An estimation of the energy content in high energy protons based on these γ-ray observations will be published in another paper (Emslie et al., 1999).

Decimetric radio emission (1.4 GHz) was also observed for this event (Fig. 9). Two rather symmetric peaks are shown, with a maximum flux of 500 sfu[7]. The first peak is around 14:58:20, slightly after the hard X-ray maximum and the second is around 15:00:50, slightly before the H_α maximum. With the exception of the second peak, the radio emission time profile is very similar to the hard X-ray one.

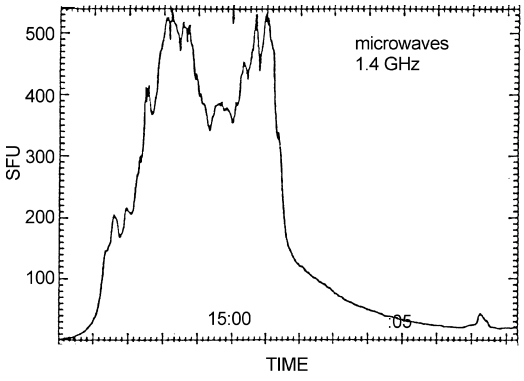

Fig. 9. Time evolution of the microwave emission (1.4 GHz) for the 1989, June 20 flare, from 14:55 to 15:08 UTC.

[7] Solar Flux Unit: 1 sfu = 10^{-22} W.m^{-2}

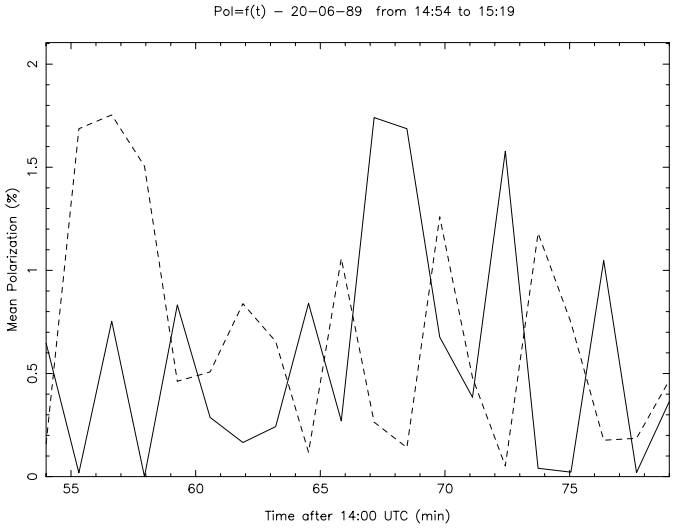

Fig. 10. Time evolution of the radial (plain line) and tangential (dotted line) components of the polarization integrated over the flare of June 20^{th} 1989, from 14:54 to 15:19 UTC.

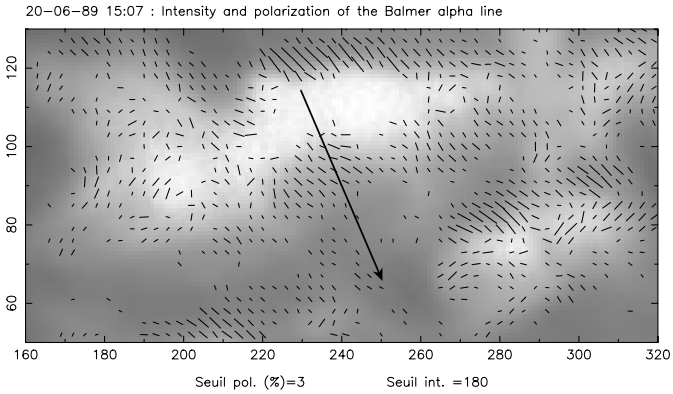

Fig. 11. H_α intensity and polarization exceeding 3% on the 1989, June 20 flare at 15:07 UTC. The radial orientation is indicated by the big arrow; the units are in pixels (≈ 0.8 arcsec). Invalid polarization data corresponding to the brightest parts of the flare have been removed.

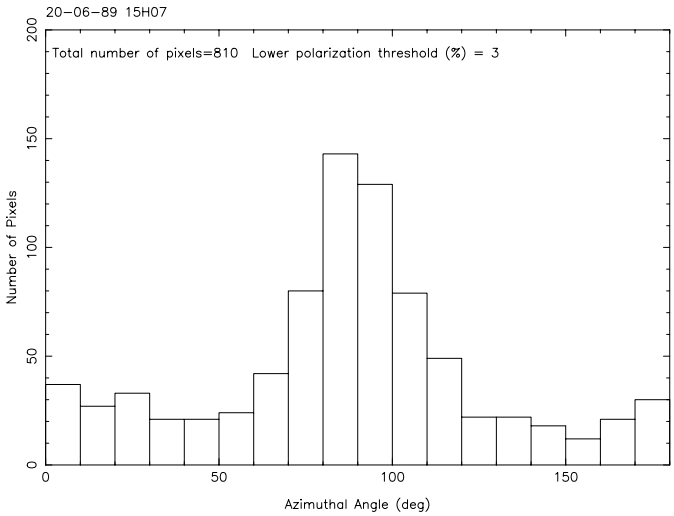

Fig. 12. Azimuth distribution of the one minute time integrated polarization exceeding 3% on the 1989, June 20 flare at 15:07 UTC. The radial orientation is at 68° and the tangential one at 158°.

4.2.3. H_α line polarization

For this event, H_α polarization was studied from 14:54 to 15:19 UTC with a time resolution of 1, 4 and 8 minutes. As for the 1982 events, the one minute integrated data are very noisy. The time profiles of the radial and tangential component of the area integrated polarization are presented in Fig. 10. The mean value of the radial component (plain curve) is 0.6% with a standard deviation of 0.5%. For the tangential component (dotted curve), the main value is 0.7% with a standard deviation of 0.5%. The tangential component is clearly dominant at the beginning of the flare, especially from 14:55 to 14:58 where it exceeds 1.5%. This corresponds to the rising and the maximum of the impulsive hard X-ray emission. Later in the flare, there are more fluctuations but the radial component appears to dominate. This is quite clear from 15:07 to 15:08 – at and just after the maximum of soft X-ray emission – and more marginally at 15:12.

The polarization map and azimuth distribution histogram for 15:07 have been represented on Figs. 11 and 12. The preferred orientation is approximately 20° from the radial direction and covers most of the flare area, with the exception of the brightest parts. This is actually an artifact due to overexposure of the film; we don't have valid polarization data for the brightest parts of this flare.

Integrated over four minutes, a tangentially dominant polarization appears at the beginning of the impulsive phase. Around the maximum of soft X-ray emission, the polarization is close to radial (main direction is 20° from the solar vertical) and near the feet of the H_α flare loop, some polarization vectors seem to be aligned with the magnetic field lines materialized by this loop. The polarization is relatively stable over the area, with a polarization degree between 3 and 5%.

The azimuth distribution for the 8 minutes integrated data is shown on Fig. 13. Although the dispersion in azimuth angle is greater, a preferred orientation still appears in 2 out of the 3 panels. During the impulsive phase of the flare (14:54 to 15:02), the peak of the histogram is at 20–30° from the tangential direction. Then, during the beginning of the gradual phase (15:03 to 15:11), the center of the large peak, ignoring smaller spikes, is at 20–30° from the radial direction. After that, during the decay phase (15:12 to 15:19), no preferred orientation appears.

4.3. Common characteristics of the observed events

The 1982 and 1989 events clearly show common characteristics for the observed H_α polarization:

– With the exception of the impulsive phase (and the decay phase for the 1989 event), the azimuth of the polarization vector is close to the radial direction on the solar disk.
– The radial polarization is more visible immediately around the maximum of soft X-ray emission and so is clearly cor-

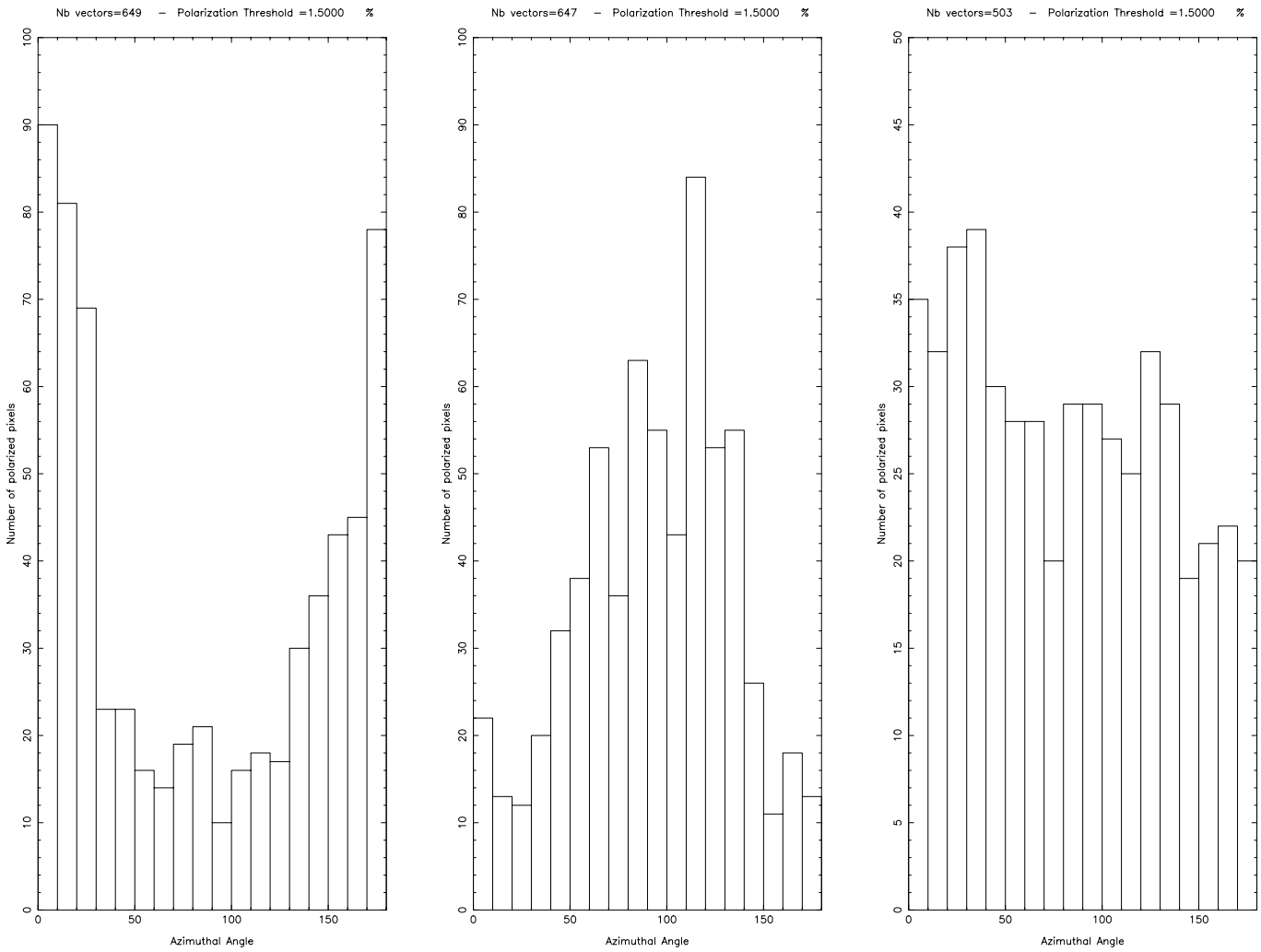

Fig. 13. Azimuth distribution of the 8 minutes time integrated polarization exceeding 1.5% on the 1989, June 20 flare from 14:54 to 15:02, 15:03 to 15:11 and 15:12 to 15:19. The radial orientation is at 68° and the tangential one at 158°.

related with a phase of heating of the atmosphere. No high energy electrons are present at that time, as indicated by the absence of hard X-ray or radio emission.

It is worth noticing that other observations also show radial polarization of the H_α line in flares, like those we cited in the introduction. Moreover, observations made in Irkutsk (Russia) along the profile of the H_α and H_β lines (Firstova et al., 1997) also show radial polarization in the H_α line for several flares.

5. Origin of the observed polarization

There are different processes that could produce linear polarization in H_α during a flare. The first is Zeeman splitting (or Stark splitting) by a local magnetic field (or electric field respectively). In our case, the bandwidth of the Lyot filter (0.75 Å) is much larger than the expected splitting. Hénoux & Semel (1981) estimated that Zeeman or Stark effect could not account for more than 0.5% in the observed linear polarization. This is an order of magnitude below the observations and these sources of polarization can thus be ruled out.

Another possible process is resonance polarization, due to the radiative excitation of the $n = 3$ level by an anisotropic Ly_β radiation field. This would produce circular patterns of linear polarization around the bright Ly_β patches with a dominant contribution in the tangential direction due to projection effects (Hénoux, 1991). Such circular patterns are not seen in our data. Furthermore, the Ly_β line is expected — as shown by the atmospheric models — to be optically thick at the H_α formation level. This rules out any significant anisotropy in the Ly_β radiation field at this level. Thus, resonance polarization as a source for the observed polarization also has to be rejected.

Then, we are left with impact polarization as the most plausible explanation for our observations. Impact polarization is due to the collisional excitation of atoms by particles with an anisotropic velocity distribution. If the energy of the exciting particles is below a critical value E_c, the emitted light will be polarized along the direction of anisotropy. For energies above E_c, the polarization is perpendicular to the plane defined by the line of sight and the direction of anisotropy. In the case of the hydrogen H_α line, the critical energy E_c is about 150 eV for elec-

trons and about 150 keV for protons (Vogt & Hénoux (1996), Vogt (1997)). If the particles are moving along an essentially vertical magnetic field, low energy particles ($E < E_c$) will give radial polarization whereas high energy particles ($E > E_c$) will give tangential polarization. The polarization degree is maximal when the emitted light is observed at 90° from the direction of anisotropy. When observed at an angle $\theta \neq 90°$ from this direction, the polarization degree $P(\theta)$ is related to the maximum polarization $P_{90°}$ by (Hénoux et al., 1983b):

$$P(\theta) = P_{90°} \frac{\sin^2\theta}{1 - P_{90°}\cos^2\theta} \tag{8}$$

5.1. Tangential polarization observed during the impulsive phase

During the impulsive phase of the 1989, June 20 flare, the polarization has a preferentially tangential orientation. It is associated with impulsive hard X-ray and radio emission, traditionally interpreted as bremstrahlung from energetic electrons. This linear polarization could be due either to beams of electrons moving with a low pitch angle around a nearly vertical magnetic field and reaching the chromosphere with a energy greater than about 150 eV or to protons of energy $E < 150$ keV mirroring in a converging magnetic field.

Since for electrons as well as for protons the energetic particle number density function and the hydrogen atomic level 3 excitation cross-section decrease with energy, the most efficient particles in the formation of the H_α line are the particles of lower energy able to efficiently collisionally excite the hydrogen level 3, i.e. 10 to 50 eV electrons and 10 to 100 keV protons. If the low energy threshold E_{thr} of the electrons energy distribution function in the corona is lower than a threshold energy E_i derived below, these electrons are isotropised in Coulomb collisions with the background thermal plasma (μ = 0 for $E_i \simeq$ 25 keV in Eq. (11)). The H_α line will then be unpolarized.

5.1.1. Electron beam

If the observed polarization is due to electrons, the polarization degree of the order of 5% implies that electrons of energy above 150 eV must be present at the H_α line formation level with a still highly directive velocity distribution function and be dominant in the energetic electron population. This condition can be used to estimate the energy E_i these electrons must have had at their injection site in the corona. After going through a column density N (in particles per cm^2), the change in pitch angle cosine μ is given by (Emslie, 1978):

$$\frac{\mu}{\mu_i} = \left[1 - (2 + \frac{\beta}{2})\frac{\gamma K N}{\mu_i {E_i}^2}\right]^{\frac{\beta}{4+\beta}} \tag{9}$$

with

$$\beta = 2\,\frac{x\Lambda + (1-x)\Lambda''}{x\Lambda + (1-x)\Lambda'} \quad , \quad \gamma = x\Lambda + (1-x)\Lambda' \tag{10}$$

where $x = \frac{N_{H+}}{N_{H+}+N_H}$ is the hydrogen ionisation degree, Λ, Λ' and Λ'' are Coulomb logarithms (≈ 10 for electrons) and $K = 2\pi e^4 = 33.43\ 10^{-38}$ (cgs). For an electron beam initially vertical ($\mu_i = 1$) propagating in a fully ionized atmosphere ($x = 1$), we get:

$$\mu \approx \left(1\text{–}10^{-35}\frac{N}{E_i^2}\right)^{1/3}, \tag{11}$$

giving for the initial energy:

$$E_i = \sqrt{\frac{N}{10^{35}(1-\mu^3)}}. \tag{12}$$

The H_α line is formed around a column density of $N \approx 1.8\ 10^{20}$ cm^{-2}, so in order to get a directivity such that the electron pitch angle cosine μ is still greater than 0.9 at this level, we need an injection energy $E_i > 50$ keV. In other words, at the coronal excitation site, the lower energy boundary E_{thr} of the energetic electrons energy distribution function must be greater than 50 keV.

5.1.2. Proton beam

In contrast to electrons, due to their higher mass, protons can reach the chromosphere with a still anisotropic velocity distribution function and be at the origin of impact polarization both in the impulsive and gradual phase of a solar flare. It may then be possible that the sign of polarization of the Balmer H_α line in the impulsive phase of solar flares depends on the magnetic field topology and on its evolution during the flare development.

As discussed in the conclusion, the particle loss cone may have a higher aperture at the flare beginning, making protons to mirror. If this mirroring takes place in the upper chromosphere, tangential linear polarization could be generated. Another possibility is that there are in the impulsive phase still magnetic field lines highly twisted around a nearly vertical direction. Protons moving parallel to them would move mainly horizontally. However, in that case, in order to penetrate into the chromosphere, these protons must have in the corona an energy higher by a factor $\sqrt{1/\mu}$ than the initial energy E_i required from protons moving vertically.

Protons drifting horizontally across vertical magnetic field lines have been suggested by some current closure models (Emslie & Hénoux, 1995) as a possible source of impact polarization. However, as the drift energy of these protons is supposed to be of the same order as their thermal energy (≈ 1 eV), it would be below the excitation threshold of the hydrogen $n = 3$ level.

High energy protons ($E_i > 1$ MeV) moving vertically could also generate tangential linear polarization. However, this would require that they are not accompanied by a greater number of lower energy protons ($E_i < 500$ keV). More probably, the proton energy distribution would keep rising below 500 keV and the net polarization produced would be radial.

5.2. Radial polarization observed during the gradual phase

Radial polarization is observed around the maximum of soft X-ray emission for both events. There are three possibilities to explain this polarization: X-ray irradiation creating anisotropic photoelectrons, particle beams from the corona or local acceleration of the background particles.

5.2.1. X-ray irradiation

Soft X-ray (typically of a few keV) are heavily emitted by the hot plasma generated in solar flares. This irradiation generates photoelectrons expelled from the inner shells of atoms like C, N and O. The photoelectron production rate is maximum in the upper solar chromosphere around the H_α formation level (Hénoux & Nakagawa, 1977). Photoelectrons are preferentially emitted in the plane perpendicular to the X-ray propagation direction; consequently, the photoelectrons produced would move preferentially in the horizontal plane and since they have an energy of a few keV, well above the turnover value, they should produce a radial polarization in the H_α line.

This process would naturally explain the correlation between the radial polarization and the maximum of soft X-ray emission. However, computations of the maximum degree of H_α polarization expected for a realistic photoelectron distribution show that this polarization is far too low (Hénoux & Karlický, 1999).

5.2.2. Particle beams

Radial polarization can be produced by vertical particle beams – protons or electrons – with an energy below the critical value E_c. Low energy electrons ($E < 150\,\mathrm{eV}$) can be immediately rejected as they would not be able to reach the H_α formation layers, so low energy protons ($E < 150\,\mathrm{keV}$) are the best candidates and their effects are discussed below.

If the protons are moving along the vertical, the maximum polarization would be observed at 90° from the beam. This would be the case for a flare observed at the solar limb. Indeed, the 1989 event, which is closer to the limb than the 1982 one, shows a higher polarization degree. Using Eq. (8), we can get the maximum polarization degree P_{90°, that we would see if the flare was located at the solar limb. For both events, around the time of maximum soft X-ray emission, P_{90° is between 2.5 and 6.5%.

In a previous paper (Vogt et al., 1997), that took into account the depolarizing effects of the background thermal particles and of the radiation field, supposed to be isotropic and unpolarized, the polarization degree that would be created by a vertical beam of protons was estimated. This degree of polarization was found to be dependent on the atmospheric temperature model used. The pre-flare atmospheric model VAL F (Vernazza et al., 1981) leads to a maximum polarization of 3% for a proton flux of $10^{16}\,\mathrm{cm}^{-2}.\mathrm{s}^{-1}$ whereas the thermal flare atmospheric model F1 (Machado et al., 1980) predicts the maximum polarization degree to be below 1%.

Although a bit low, the first result is compatible with the observed polarization. This slight discrepancy can be explained by some weaknesses in the theoretical model used. Firstly, the proton-hydrogen collision cross sections used were rather crude. There are now accurate close-coupling cross sections available (Balança, 1997), (Balança & Feautrier, 1998) and new computations are in progress. Also, these computations were done with an unpolarized radiation field. Since a significant part of this radiation field comes from the energy deposited by the non-thermal protons, polarization in the radiation field should be taken into account in a self-consistent way. This would presumably produce a higher polarization degree.

The fact that the polarization degree obtained by using empirical thermal flare models is an order of magnitude below the observed polarization strongly recall us that these models are not the most suitable to describe a non-thermal flare. In order to get a polarization degree in agreement with the observations, the electron density in particular should be lower at the H_α formation level than the one given by the F1 model.

Fang et al. (1993) and Hénoux et al. (1993) have shown that non-thermal excitation and ionization of the atmospheric hydrogen by the particles of a beam strongly increase the intensity of chromospheric lines like the Balmer H_α line. This conclusion is valid whatever the type of beam particles, electrons or protons, i.e. even if there is no evidence for an impulsive phase. Proton beams with, at the acceleration site in the corona, an energy dependance of the proton number flux above 150 keV given by a power law $\mathrm{E}^{-\delta}$ were found to generate significant hydrogen non-thermal excitation and ionization. For a thermal atmosphere represented by the empirical flare model F1, as soon as the energy flux carried was equal to or higher than $10^{10}\,\mathrm{erg.cm}^{-2}.\mathrm{s}^{-1}$ and whatever the value of the power index δ used, the Balmer H_α intensity line profile became comparable to the one predicted by the purely thermal flare model F2.

Indeed the thermal empirical flare model F1 used by Fang et al. (1993) and Hénoux et al. (1993) is still more dense and hot than the model VAL F used in this paper. However, the dominance of the non-thermal processes is such that adding them to the thermal processes associated to empirical plage model VAL F would have led also to a Balmer H_α intensity line profile comparable to the ones predicted by purely thermal flare models, like F1 and even presumably F2.

In the classical model, where all flare energy is deposited during the impulsive phase, the soft X-ray emission just results from the relaxation of the hot thermal plasma remaining after the particle bombardment has stopped. In the 1989 June 20^{th} flare for which hard X-ray observations are available, the maximum of soft X-ray emission takes place near the end of the hard X-ray emission and seems to vary as the total time integrated flux of hard X-rays. However, radial linear polarization is most evident just after the maximum of soft X-ray emission when there is no more electron bombardment. At that time, protons are still bombarding the chromosphere, either being still accelerated into the corona or more probably just leaking from the coronal magnetic trap, where they were injected previously, into the lower atmosphere.

On the sun, magnetic fields are not always vertical, so we expect some spatial variation in the proton beam direction, which will be reflected on the polarization vector azimuth. Such effects are observed since the main orientation of the polarization sometimes differs from the radial direction by 10 or 20 degrees. In particular, on the 1989 flare, we see at some times near the feet of the H_α flare loop, polarization vectors that are aligned with the magnetic field lines traced out by this H_α flare loop. This is a strong indication that particles moving along the magnetic field lines are responsible for this polarization.

5.2.3. Local acceleration

Local acceleration of the background particles could lead to an anisotropic velocity distribution of the ambient electrons and protons. Such an acceleration could be realised by a local charge distribution called *electrostatic double layer* where two regions of opposite electric charge are encountered over a short distance. The voltage between the two layers is able to accelerate local particles to energies of a few eV (weak double layer) to a few tens of keV (strong double layer). These double layers were introduced in the frame of flare models based on the dissipation of electric currents (Alfvén & Carlqvist, 1967).

The local acceleration of protons to the energies of a few keV required for sufficient excitation of the $n = 3$ level requires the formation of a strong double layer. This is quite unlikely in the conditions of the solar atmosphere (Hénoux, 1987). On the other hand, a series of weak double layers in the upper chromosphere could accelerate ambient electrons to an energy of some tens of eV, sufficient for H_α excitation. However, their formation requires current concentrations on a spatial scale of the order of 10 km, that current telescopes are unable to resolve.

Anisotropic electrons of a few tens of eV accelerated locally by weak double layers could create an impact polarization less sensitive to the depolarizing effect of collisions with thermal particles, as a great proportion of these would be accelerated. However, this hypothesis cannot easily explain the association between the radial polarization and the soft X-ray emission.

Conclusion

The observations presented in this paper confirm the existence of a linear polarization of the H_α line during solar flares. The polarization degree is between 2 and 6%, the orientation is essentially radial – directed towards the disk center – and the polarization is more clearly observed around the maximum of soft X-ray emission, during the gradual phase of the flares. A tangential orientation – parallel to the solar limb – also appears during the impulsive phase of one of the events, in association with the hard X-ray emission, but with a high level of noise.

Tangential linear polarization is present at the very beginning of the rise of the H_α line intensity, and is associated with the rise of hard X-ray emission, i.e. with atmospheric bombardment by high energy electrons. If confirmed, it could be due either to beams of electrons with an initial energy greater than about 50 keV bombarding the chromosphere and responsible for hard X-ray emission, or to low energy protons ($E < 150$ keV) mirroring in a converging magnetic field. It must also be recalled that a predominant radial direction was found for the linear polarization present during the impulsive phase of the two flares observed by Metcalf et al. (1992) and (1994).

Since the energetic particles', electrons or protons, number density $N(E)$, per energy band dE, and the hydrogen atomic level 3 excitation cross-sections decrease with energy, the most efficient particles in the formation of the H_α line are the 10 to 50 eV electrons and the 10 to 100 keV protons present at chromospheric level. Among these two populations, in the presence of Coulomb collisions with the background thermal plasma, only protons are left with a still anisotropic velocity distribution function, both in the impulsive and progressive phase of a solar flare. Extension of the energy distribution of the electron number density in the corona downwards to energy below 50 keV would lead to unpolarized Hα emission.

It may then be possible that the sign of polarization of the Balmer H_α line, in the impulsive phase of solar flares and later, depends on the magnetic field topology and on its evolution during the flare development. It is widely admitted that the energy released in solar flares comes from the magnetic field evolution by dissipation of its non-potential component. Consequently, in the scenario where the flare energy release takes place in the corona, we can assume that coronal magnetic fields in a flaring active region decrease during the flare and that the loss cone aperture angle θ, such that $\sin^2\theta = B_c/B_{ch}$, where B_c and B_{ch} are respectively the coronal and chromospheric magnetic fields, decreases with time. This would make the proton velocity distribution function in the upper chromosphere more directed along the main chromospheric magnetic field direction with time, leading consequently to a radial or nearly radial direction of polarization during the flare progressive phase. During the impulsive phase, the direction of polarization would be more sensitive to the local conditions that vary from flare to flare and could be sometimes longitudinal, sometimes radial.

A careful energy evaluation would be required in order to determine if the observed time extension of the H_α line brightness beyond the impulsive phase requires continuous particle acceleration or not, or could be explained by a leak into the chromosphere of low energy protons trapped in magnetic structures, whatever the time of their acceleration.

Rather than generating the observed H_α line polarization by primary particle beams, Fletcher & Brown (1998) suggested that this polarization results from interaction between chromospheric hydrogen and an evaporating plasma, at the boundaries between these two components. However, such evaporation requires a continuous energy deposit, the effects of which cannot be a priori ignored. As a matter of fact, this source of energy deposit may well be proton beams.

The computations of the H_α line degree of polarization, that have been done in the hypothesis of hydrogen impact excitation by protons by Vogt et al. (1997) have shown that the net degree of polarization depends on the local background plasma density. This is coherent with the observation that, as Fig. 10 and Fig. 7 show for the 1989 June 20 flare, radial polarization is

present mainly at times where the H_α line brightness decreases. The intermixing of the direct contribution of protons in generating linear impact polarization by hydrogen excitation and of their indirect and opposite effect of reducing the amplitude of this polarization by increasing the local electron number density, makes it difficult to draw definitive conclusions about the time evolution of the number density of the low energy proton population in solar flares from the study of two events.

In order to know if the polarimetric characteristics reported here are common to a great number of solar flares, or if they affect only a limited class of events, new observations are needed. Indeed, it would be also extremely interesting to obtain simultaneous observations of H_α polarization and γ-ray lines intensities, in order to derive the proton spectrum from low to high energies. Systematic observations of H_α polarization in solar flares at Meudon are planned with the new PARIS polarimeter.

References

Alfvén H., Carlqvist P., 1967, Solar Physics 1, 220
Balança C., 1997, Ph.D. thesis, Paris XI University
Balança C., Feautrier N., 1998, A&A 334, 1136
Emslie A., 1978, ApJ 224, 241
Emslie A., Hénoux J.-C., 1995, ApJ 446, 371
Emslie A., Miller J., Vogt E., Hénoux J.-C., 1999, (in preparation)
Fang C., Hénoux J.-C., Gan W., 1993, A&A 274, 917
Firstova N., Hénoux J.-C., Kazantsev S., Bulatov A., 1997, Solar Physics 171, 123
Fletcher L., Brown J.-C., 1998, A&A 338, 737
Hénoux J.-C., 1987, in V. Stepanov, V. Obridko (eds.), Solar Maximum Analysis, pp 109–122, VNU Science Press, Utrecht
Hénoux J.-C., 1991, in L. November (ed.), Solar Polarimetry, 11th NSO/Sac Peak workshop
Hénoux J.-C., Chambe G., 1990, J. Quant. Spectrosc. Radiat. Transfer 44, 193
Hénoux J.-C., Karlický M., 1999, A&A 341, 896
Hénoux J.-C., Nakagawa Y., 1977, A&A 57, 105
Hénoux J.-C., Semel M., 1981, in V. Obridko, E. Ivanov (eds.), Proceedings of the Crimea Solar Maximum Year Workshop, pp 207–210
Hénoux J.-C., Chambe G., Semel M., Sahal S., Woodgate B., Shine D., Beckers J., Machado M., 1983a, ApJ 265, 1066
Hénoux J.-C., Chambe G., Smith D., Tamres D., Feautrier N., Rovira M., Sahal-Bréchot S., 1990, ApJS 73, 303
Hénoux J.-C., Fang C., Gan W., 1993, A&A 274, 923
Hénoux J.-C., Heristchi D., Chambe G., Machado M., Woodgate B., Shine R., Beckers J., 1983b, A&A 119, 233
Machado M., Avrett E., Vernazza J., Noyes R., 1980, ApJ 242, 336
Metcalf T., Mickey D., Canfield R., Wulser J.-P., 1994, in High Energy Solar Phenomena, Vol. AIP Conf Proceedings 294, pp 59–63
Metcalf T., Wulser J.-P., Canfield R., Hudson H., 1992, in The Compton Observatory Science Workshop, Vol. NASA Conf Proceedings 3137, pp 536–541
Murphy R., Ramaty R., Kozlovsky B., Reames D., 1991, ApJ 371, 793
Ramaty R., Mandzhavidze N., Kozlovsky B., Murphy R., 1995, ApJ 455, L193
Share G., Murphy R., 1995, ApJ 452, 933
Simnett G., 1995, Space Sci. Rev. 73, 387
Vernazza J., Avrett E., Loeser R., 1981, ApJS 45, 635
Vogt E., 1997, Ph.D. thesis, Paris VII University
Vogt E., Hénoux J.-C., 1996, Solar Physics 164, 345
Vogt E., Sahal-Bréchot S., Hénoux J.-C., 1997, A&A 324, 1211